

RADIATION HEATING IN SUPERCONDUCTING MAGNETS
AND PROTON BEAM LOSS LIMITATIONS

M.A. Maslov and N.V. Mokhov,
IHEP, Serpukhov, USSR

ABSTRACT

Following the example with superconducting magnets of the IHEP accelerating and storage complex (UNK) the accelerating proton beam loss limitations due to radiation heating in superconducting windings are treated. Regularities of formation of energy release fields in dipole magnets irradiated diversely by 200-3000 GeV protons have been investigated. The three-dimensional nuclear-electromagnetic cascades have been calculated by the Monte-Carlo method with the MARS-6 programme with account for the magnetic azimuthal structure and the field in the aperture and superconducting windings. Factors determining the values of tolerable accelerator particle losses in the superconducting magnets have been considered. Proton loss limitations in the UNK superconducting ring have been estimated for some model cases. Additional heat loadings on the cryogenic system have been shown to be a factor influencing the value of tolerable losses.

I. INTRODUCTION

Beam-bending and focusing superconducting magnet systems (SMS) are the heart of the accelerating complex projects of the generation to come^{1, 2)}. Since proton losses at various stages of the accelerator cycle are inevitable superconducting magnets will be functioning under continuous influence of ionization radiation. The energy released in the magnet elements during the development of nuclear-electromagnetic cascades results in the radiation damage of materials, quench of superconducting windings and additional heat loadings on the cryogenic system. Without special measures being taken, the radiation heating of SMS is, unquestionably, the basic reason limiting the beam design intensity at new accelerators.

The estimates of tolerable values of energy deposition density in the windings and, correspondingly, specific particle losses have been obtained in early papers⁴⁻⁸⁾ devoted to radiation heating. Since the limitations on the losses are very grave, and considerable simplifications have been made in the above mentioned papers, it becomes necessary to treat this problem as seriously as possible, with account for all the principle factors influencing quench of superconducting windings.

The present paper attempts to solve this problem by the example with the superconducting magnets of the IHEP accelerating and storage complex (UNK). As differed from the previous works, it investigates the regularities of formation of energy deposition fields

in the SMS under various conditions of irradiation, covering the majority of actual situations. Monte-Carlo calculation of the three-dimensional nuclear-electromagnetic cascades have been made with the MARS-6 programme, which considers the azimuthal structure of the magnet and beam losses in the magnet cross section and also the influence of the aperture and magnet winding field on the cascade development. Based on the obtained data, the tolerable heating and proton losses are estimated.

II. THE UNK SUPERCONDUCTING MAGNETS

As an example, we shall treat the problem of the SMS radiation heating in the UNK dipole magnets²⁾. A two-stage proton accelerator of the maximum energy of 3000 GeV is planned to be installed in the UNK tunnel 19,2 km long. The first stage with warm electromagnets will stack 10-12 pulses from the U-70, $5 \cdot 10^{13}$ protons in pulse, and will accelerate them to 400 GeV. Then a $(5-6) \cdot 10^{14}$ proton beam will be accelerated up to the maximum energy in the second stage comprising cold magnets.

A UNK superconducting dipole magnet is a shell-type one 6 m long. The magnet model, as it is accepted in the present calculations, is shown in Fig. 1. A superconducting two-lamination winding (SCW) is formed by a flat cable from single transposed conductors manufactured from 10 μ m filaments, embedded in a copper matrix in this NbTi/Cu = 1. At the maximum energy of protons the induction in the centre of the vacuum chamber is 5 T.

As was assumed in the calculations, each lamination of the winding is to be cooled by one-phase helium flow around the ring channels. For a two-lamination winding the number of such channels is three. The helium and winding temperature without the radiation fields lies within 4,2-4,6^oK, and its final value will be chosen after detailed calculations of the operation costs of the cryogenic system as a whole. In the present calculations this temperature was accepted to be equal to 4,5^oK.

III. THE COMPUTER PROGRAMME

When high energy particles interact with the vacuum chamber, a nuclear-electromagnetic cascade occurs in the magnet elements. The energy deposition value and its dynamics in the process of the cascade development determine the temperature fields in the SMS,

The three-dimensional cascades are calculated by a Monte-Carlo method in terms of the MARS⁹⁻¹¹⁾ computing complex. When simulating hadron-nuclear interactions an inclusive approach is applied. The hadron primary energies are within the range of 20 MeV-3000GeV.

The peculiarities of simulation, the physics model, the calculational algorithm for all the processes resulting in the energy deposition, the geometric and servicing facilities are described in detail in papers¹⁰⁻¹¹⁾. Here we shall present a brief description of a new version of the MARS complex, the MARS-6 programme. Note that the previous version, MARS-5, additionally calculates spatial-energy and angular distributions of p, n, π^+ , π^- , K^+ , K^- , \bar{p} as well as the stopping densities of negative hadrons (π^- , K^- , p, Σ^- , ...) ¹²⁾.

The MARS-6 programme, conserving all the facilities of MARS-4¹¹⁾, makes it possible to consider the field effect and also the azimuthal structure of the magnet and the beam losses in its cross section. A magnet is set as a cylinder with inner bounds in the form of coaxial cylindrical surfaces with plates arbitrary divided in length and azimuth, and may consist of an arbitrary combination of three materials, each being a mixture of up to six matters (A = 1-238). There may be present the vacuum cavities.

A change of charged particle trajectories, under the influence of the field in the matter and vacuum, is taken into account. The MARS-6 programme applies the algorithm of simulating the charged particle trajectories in the limited media with the fields of an arbitrary form¹³⁾. Simulation is performed numerically by the broken spiral method. The estimates show that in most of the cases multiple Coulomb scattering influences weakly the formation of the energy deposition field in a superconducting winding. Therefore we did not take this process into account in the present work.

The field induction distribution can be given by a table or a formula. In the case of a homogeneous field in the magnet aperture only, the motion equation is integrated analytically. The algorithm enables to take into account the presence of an electromagnetic field as well.

IV. SMS IRRADIATION CONDITIONS

The spatial distributions of energy deposition density in the elements of a superconducting magnet, described in Section II, have been calculated by the MARS-6 programme. The losses of protons $E_0 > 200$ GeV on the magnet string have been considered. The coordinate origin has been placed in the centre of the left edge of the first magnet (see Fig. 1). Four cases of irradiation have been singled out.

Case 1. An incident proton beam of infinitesimal lateral extent hits at a fixed angle θ the vacuum chamber in the point with the fixed coordinates $\vec{r}^{\rightarrow}(0; 3,5; 0)$, $\phi = \pi/2$. This is the most general case; the combination of such solutions yields a result in the case of arbitrary irradiation. The most complete information has been obtained just for this ver-

sion. To make the picture complete, other versions of losses have been considered.

Case 2. The result is the same as for case 1, but the losses are linear along the magnet length. The case simulates particle losses in a residual gas, the losses of finite dimension beam incident in the vacuum chamber at small angles, irradiation of SMSs installed at a long distance from the local sources.

Case 3. The proton beam density is distributed normally

$$p(x, y) = \frac{1}{\sqrt{2\pi}\sigma(E_0)} \exp\left(-\frac{x^2 + y^2}{2\sigma^2(E_0)}\right), \quad (1)$$

where $\sigma(E_0)$ is the dispersion dependent on proton energy. For the second stage of the UNK we have the following approximate dispersion $\sigma(E_0) = 0,2\sqrt{1500/E_0}$ cm. Such a beam is centered at $\phi = \pi/2$ and is incident in the vacuum chamber at a fixed angle θ .

Case 4. A beam interacts with a point target placed at various distances from the magnet. The efficiency of the target is 100%. This case simulates SMS irradiation by particles generated by any local source: targets, scrapers, electrostatic septa.

In all the cases the differential energy deposition density, $\epsilon(z, r, \phi)$, has been calculated in the cylindrical coordinate system, the field being present and absent in the magnet. The distributions averaged over azimuth,

$$\epsilon_1(z, r) = \frac{1}{2\pi} \int_0^{2\pi} \epsilon(z, r, \phi) d\phi, \quad (2)$$

the maximum energy deposition density, ϵ_M , in the "hottest" point of the superconducting winding and a number of other functionals have also been calculated.

The investigated range of beam incident angles to the vacuum chamber is $0 < \theta < 10$ mrad, what must deliberately exceed a possible range of θ variation in the second stage of the UNK. The most probable value of θ is supposed to be 1 mrad. Therefore a large number of regularities have been obtained for this very value.

V. FORMATION OF ENERGY DEPOSITION FIELDS IN SMS. CALCULATIONAL RESULTS.

This section presents some calculational results of energy deposition fields in the superconducting windings (SCW) of the magnets at the proton energy of $E_0 = 200 - 3000$ GeV. The statistical inaccuracy of the results is $< 25\%$. The data have been normalized for one incident proton.

Figs. 2-5 present the distribution of the differential energy deposition density, $\epsilon(z, r, \phi)$, in SCW with the local losses of proton beam of infinitesimal lateral extent in the vacuum chamber (case 1). In the energy range under investigation the shape of the longitudinal distributions is almost independent of energy. The maximum and its value are

determined by the values of angles θ and ϕ (Fig. 2). The maximum value of the energy deposition density, ϵ_M , is linearly proportional to the energy.

Separate histograms shown in the Figures reflect the influence of the field on the spatial distributions of the energy deposition density. Our calculations have shown that in all considered cases of irradiation (except case 4) the maximum energy deposition density at $B \neq 0$ increases by a factor of two. Therefore to save the computer time in a number of cases the calculations have been performed for $B = 0$. Note that in the case of losses under consideration the effect is determined almost completely by the field value in the magnet aperture and a slight difference from homogeneous field influences the result weakly.

The shape of radial (Fig. 4) and azimuthal (Fig. 5) distributions of energy deposition on the magnet cross section is weakly dependent on the energy of the particles lost. The value of $\epsilon_1(z, r)$ (2) was calculated in earlier papers. From Figs. 4, 5 where $\epsilon_M \approx 10\epsilon_{M0}$ the necessity to take into account the azimuthal structure when considering radiation heating follows quite obviously.

The calculations have shown that with the values of $E_0, \theta, \sigma(E_0)$ both radial and azimuthal distributions of $\epsilon(z, r, \phi)$ in the magnet SCW are of practically the same form for the irradiation conditions under investigation (cases 1-4). This conclusion holds true at least for the most important range of the maximum of longitudinal distributions. In this sense Figs. 4, 5 have a very general character.

As was already stated, the distribution of the energy deposition density along the magnet length is greatly dependent on the initial conditions. Fig. 6 presents the longitudinal distributions of energy deposition in the windings with the losses of proton beam distributed according to (1) in the chamber (case 3). At $\theta > 5 \cdot 10^{-3}$ the case of beam losses with the Gaussian distributions of density (1) is practically identical to that of the local losses of a beam of infinitesimal lateral extent and at $\theta < 3 \cdot 10^{-4}$ it is identical to the case of linear losses.

Fig. 7 illustrates the dependence of the maximum energy deposition density on the dispersion of beam density distribution (1) for the case of $\theta = 10^{-3}$. This dependence can be approximated by the expression

$$\frac{\epsilon_M(\sigma)}{\epsilon_M(\sigma=0)} = 0,5 e^{-\sigma/0,4} (1 + e^{-\sigma/0,072}), \quad (3)$$

where $0 < \sigma < 0,5$ cm, $\theta \approx 10^{-3}$.

The calculational results of the maximum energy deposition density in SCW versus the angle of a beam incident on the vacuum chamber are presented in Fig. 8, in which the data

for the energies of $E_0 = 400 - 3000$ GeV are accumulated (cases 1 and 2). One can note a fairly weak angular dependence at $\theta < 2 \cdot 10^{-3}$ and a sizable increase in energy deposition versus an angle for $\theta > 2 \cdot 10^{-3}$. Bearing in mind a 25% error of the results and neglecting the difference in the data for local and uniform losses, one can approximately describe the angular dependence of the maximum energy deposition density in the windings by the following expression

$$\epsilon_M(\theta)/\epsilon_M(\theta_0) = 0,9 \left(\frac{\theta}{\theta_0}\right)^{0,352} + 0,1 \left(\frac{\theta}{\theta_0}\right)^{2,236}, \quad (4)$$

where $\theta_0 = 10^{-3}$, $10^{-4} < \theta < 10^{-2}$ rad.

In the present work all the calculations have been made for the total thickness of the magnet steel constructions inside the SCW of 0,15 cm (effective "vacuum chamber"). For other thickness the value of the maximum energy deposition density in the SCW can be determined from Fig. 9 which shows the data for the uniform proton losses at various incident angles. The obtained function $\epsilon_M(d)$ is essentially dependent on the angle θ rather than on the energy E_0 and irradiation conditions, with large values of d the curves behave in the same way. With $\theta = 10^{-2}$ the following approximation

$$\epsilon_M(d) = 4,3 e^{-d/d_0} \text{ GeV} \cdot \text{g}^{-1} \cdot \text{prot}^{-1} \cdot \text{m} \quad (5)$$

where $d_0 = 0,15$ cm, $0,15 < d < 0,8$ cm, can be applied for estimates.

As seen from the Figure, the metal shielding outside the windings is a possible protection measure for the SMS against the irradiation.

Superconducting magnet heating caused by the local source radiation is of particular interest (case 4). This case corresponds to proton beam losses on targets, scrapers, electrostatic septa. The field effect is rather essential in this case.

Fig. 10 gives the longitudinal distribution of the energy deposition density in the Doubler superconducting dipole¹). Within a distance of $D = 20$ m there is a point target with which a 1000 GeV proton beam interacts. For the sake of comparison Fig. 10 presents the calculational results for the Doubler, which agree with our data within 50%. The effect of the $B = 4,2$ T field results in 7-fold increase in the maximum energy deposition density in SCW with respect to the energy deposition maximum without the field being considered. For $z \approx 7-8$ m, which is corresponding to the second magnet in the 6 m long string of magnets, this difference is about 40-fold. It is paying attention to the second peak at $4,61 < \phi < 4,71$ caused by the fact that negative particles carry less energy due to the leading effect than positive ones.

Fig. 11 shows the maximum energy deposition density in the SCW of the UNK dipoles as a function of a distance from the target, with which a 1500 GeV proton beam interacts with

100% efficiency. The two regions with a bound at $D \approx 10$ m are rather noticeable.

During "instantaneous" proton losses (the duration of the loss pulse τ is about 1 msec) there occurs adiabatic heating, determined by the energy deposition in the "hottest" point of the winding. Extrapolating the radial distributions to the inner radius of the SCW¹⁴⁾ one can obtain the required value of the maximum energy deposition density. The energy dependence ϵ_M for the three cases of the UNK dipole irradiation at $B = 0$ are shown in Fig. 12 together with the maxima of distributions (2) integrated over the azimuth. An interesting fact of the linear growth of the maximum energy deposition density allows one to put down the following expression

$$\epsilon_M(E_0) = A \cdot E_0, \text{ GeV} \cdot \text{g}^{-1} \cdot \text{prot}^{-1}, \quad (6)$$

where E_0 , GeV is the energy of a proton incident of the vacuum chamber, $200 < E_0 < 3000$ GeV, A is the coefficient, whose values at $\theta = 10^{-3}$, $d = 0,15$ cm and $B = 0$ are equal to

$$A, \frac{1}{\text{g prot}} = \begin{cases} 6,8 \cdot 10^{-5}, & \text{case 1} \\ 7,8 \cdot 10^{-6}, & \text{case 1'} \end{cases}$$

$$A, \frac{1}{\text{g prot}} = \begin{cases} 1,4 \cdot 10^{-4}, & \text{case 2} \\ 2,1 \cdot 10^{-5}, & \text{case 2'} \end{cases}$$

for various cases of irradiation. The obtained data on the integral values of ϵ_{IM} (cases 1' and 2') coincide with the results of a previous paper¹⁴⁾. Consideration for the azimuthal structure of the distributions in the magnet cross section, $\epsilon_M / \epsilon_{M1} \approx 7-9$, is worth to be noted again.

To estimate the maximum field effect on the value of the energy deposition density ϵ_M the calculations were repeated with $B = 5$ T for all the energies. These data are shown in Fig. 12 by dashed lines. Such an overestimation is seen to yield the greatest deviation, which is equal to 50% (at $\theta = 10^{-3}$) from the cases with $B = 0$. Therefore to estimate the tolerable losses, below we used the data from (6) at $B = 0$.

In the case of single beam losses whose dispersion is governed by the law $\sigma(E_0) = 0,2 \sqrt{\frac{1500}{E_0}}$ cm, the maximum energy deposition density in the SCW at $B = 0$ is approximated by the expression

$$\epsilon_M(E_0) = 2,6 \cdot 10^{-6} E_0^{1,28}, \text{ GeV} \cdot \text{g}^{-1} \cdot \text{prot}^{-1} \quad (7)$$

at $\theta = 10^{-3}$ and $400 < E_0 < 3000$ GeV.

With the loss duration $\tau > (0,01 - 0,1)$ sec a SMS quench is determined by the mean value of the energy deposition density $\bar{\epsilon}$ in the shell of the winding (see next Section). The relation

$$\bar{\epsilon} = (0,3 - 0,4) \epsilon_M \quad (8)$$

holds true in practically all the cases.

Note that in the first and the third cases of irradiation at $E_0 > 400$ GeV, $\theta = 10^{-3}$, $d = 0,15$ cm and $B = 0$, from 20 to 35% of incident energy is deposited in the superconducting windings and bandage (low temperature part in the magnet). The remaining energy is deposited into the vacuum chambers, shieldings, reverse magnetic pipes and is carried away into the aperture by the noninteracting particles and by the secondaries through the sideways surface of the magnet.

VI. BEAM LOSS LIMITATIONS

The value of tolerable proton losses in the superconducting magnets is determined by the energy deposition density $\varepsilon(\vec{r})$ in the windings under the given irradiation conditions, the tolerable excess of the SCW temperature ΔT_M , the loss duration τ , the winding thermal and physical parameters, the cooling system and the cryogenic system facilities.

The maximum tolerable heating of a superconducting winding can be estimated from the dependence $I_c(T, B)$ of the critical current density for a magnet. The analysis of the data from^{1,15-16)} shows that with the given value of the current density I in a magnet, the maximum heating in the point of a SCW, where the field induction is of the maximum value B_M , can be found from the ratio

$$\Delta T_M \simeq (T_c - T_0)(1 - \xi'), \quad (9)$$

where $T_c = 9,5^\circ\text{K}$ is the critical temperature of the NbTi alloy in the field $B = 0$, $T_0 = 4,5^\circ\text{K}$ is the SCW temperature without radiation heating, $\xi' = I/I_c$, I_c is the magnet critical current at the temperature T_0 .

For a superconductor placed in a high field at a constant temperature the relation $I_c B \simeq \text{const}$ holds true¹⁾. Then for a tolerable heating in an arbitrary point \vec{r} of the SCW we shall have

$$\Delta T_M(\vec{r}) \simeq (T_c - T_0) \left(1 - \xi' \sqrt{\frac{B(\vec{r})}{B_M}}\right) \quad (9')$$

instead of (9), where $B(\vec{r})$ is the value of the field induction in this point with the current density in the magnet $I = I_c \xi'$. Note that in the first shell of the SCW, considered in this Section, $\max \left[\frac{B_M - B(\vec{r})}{B_M} \right] \simeq 0,1$.

The aperture field 5 T corresponding to the UNK maximum proton energy $E_M = 3000$ GeV is supposed to be reached at $\xi' = 0,85$. Putting $\xi' = 0,85 E/E_M$ into (9') one can easily find the tolerable heating of the winding at all stages of the accelerator duty cycle.

Knowing the energy deposition field $\varepsilon(\vec{r})$ in the magnet irradiated by a single beam and the tolerable heating (9'), one can obtain the maximum tolerable proton losses ΔI . For

this purpose one should solve the boundary-value problem of heat conductivity for the heat source $\epsilon(\vec{r}) \frac{\Delta I}{r}$ functioning in the winding within the period of time τ . To solve it stringently one should apply numerical method⁸⁾, yet considering the peculiarities of $\epsilon(\vec{r})$ and of the winding parameters, one can obtain an approximate solution for simple estimates.

A superconducting winding is formed by a flat cable insulated with the materials with extremely poor heat conductivity (lavsan, fiber glass). Consequently, the problem can be solved for a single cable. The cable cross section is a trapezium with about equal bases δ_1, δ_2 and the height $l \gg \delta_1, \delta_2$. On the other hand, as is seen from the previous Section, a noticeable change in the energy deposition density takes place just in the radial direction along l . All of it makes it possible to reduce the problem to solving of a one-dimensional equation of heat conductivity with a source approximately exponential along l :

The analysis has shown that due to its conductors transposed the cable heat conductivity is determined by copper. Therefore in the UNK superconducting magnets the effective cross sectional heat conductivity K , as differed from the data of papers^{5,8)} will be sufficiently high. The efficiency of heat transfer h through the cable insulation to helium is determined by the heat conductivity of insulation materials and the emission into liquid helium. The characteristic value of h is about $0,01 \text{ W/cm}^2\text{K}$. Therefore for $l \sim 1 \text{ cm}$ the ratio $h\ell/K < 0.1$ holds true. In this case, based on the solution of the heat conductivity equation, one can put down the following expression

$$\Delta H(T_M) \approx \bar{\epsilon} \frac{\Delta I}{r} r_1 (1 - e^{-\tau/r_1}) + (\epsilon_M - \bar{\epsilon}) \frac{\Delta I}{r} r_2 (1 - e^{-\tau/r_2}), \quad (10)$$

where $\Delta H(T_M) = \int_{T_0}^{T_M} C(T) dT$ is a change in the superconducting cable enthalpy, $T_M(\vec{r}) = T_0 + \Delta T_M(\vec{r})$, $C(T)$ is the effective specific heat of the cable, $r_1 = c\rho\ell/2h$ is a characteristic time of helium heat removal in the SCW (at $T_0 = 4,5^\circ\text{K}$ for pool boiling helium, $r_1 \approx 0,05 - 0,1 \text{ sec}$), $r_2 = c\rho\ell^2/(\pi^2 K)$ is a characteristic time of heat diffusion over the cable cross section ($r_2 \approx 0,005 \text{ sec}$), ϵ_M and $\bar{\epsilon}$ are respectively, the maximum and average values of the energy deposition density (6) - (8) in the length, ρ is the effective cable mass density.

Based on the data of papers^{15,16)}, we shall describe the superconducting cable enthalpy (50% Cu + 50% NbTi) with the following expression

$$H(T), \text{ J/g} = 1.12 \cdot 10^{-5} T^2 + 3.34 \cdot 10^{-2} T^4 \quad (11)$$

Fig. 13 gives the relevant enthalpy diagrams for two values of T_0 .

Note that relation (10) is valid only under the condition $r_1 \gg r_2$ resulting from the requirement $h\ell/K \ll 1$. It suggests that during "instantaneous" losses,

$$\Delta I = \Delta H(T_M)/\epsilon_M \quad (12)$$

This coincides with the case of adiabatic heating¹⁴⁾.

Considering relation (8) we shall obtain the limitations for "long-term" losses at $r \gg r_1 \gg r_2$ in the following form

$$\Delta I = \Delta H(T_M) \cdot r / (\epsilon \cdot r_1) \quad (12')$$

All the estimates presented above are valid at a slight change of the cooling helium temperature during the loss r , i.e. when the condition

$$\Delta T_{\text{He}} = \frac{q \ell}{M C_{\text{He}}} < 0,1 \quad (13)$$

holds true. Here q is the heat flow in helium from the windings per unit of the SMS length in W/m; M is the helium consumption in g/sec; ℓ is the cryogenic system length in m; C_{He} is the specific heat of liquid helium.

Fig. 14 presents the tolerable proton losses in the UNK dipole magnets at various durations of the losses pulses. The results are calculated for the cases of irradiation by Gaussian beam or that of infinitesimal lateral extent as a function of the current density in the magnet or, which is being the same, of the accelerated beam energy. In this case $E_{\text{inj}} = 400 \text{ GeV}$ ($\xi' = 0,11$) and $E_M = 3000 \text{ GeV}$ ($\xi' = 0,85$). A feasible decrease in the value of tolerable losses is observed in the process of acceleration. The results of the calculations performed by general expression (10) in the extreme cases of "instantaneous" and "long-term" losses obviously tend into (12) and (12').

Note that at $E > 400 \text{ GeV}$ the beam type, whether it is of infinitesimal lateral extent or of Gaussian type, is practically inessential for uniform irradiation. This is related to anisotropic particle scattering when they interact on the chamber and to the fact that effective dimension of a Gaussian beam with the dispersion determined in (1) is less than that of a cell size in azimuth under calculation.

It is noteworthy that the data from Fig. 14 are dependent on the maximum proton energy only via relations (6) - (8). The value of $\epsilon_M \Delta I$ is independent of the accelerator energy at least within the proton energy range of 200-3000 GeV.

The limitations on the proton losses presented in Fig. 14 correspond to requirement for any part of the winding to remain in the superconducting state. Yet, as has been shown in paper⁸⁾ that by limiting the thermal loading on the cryogenic system, for example, by the value $q = 1 \text{ W} \cdot \text{m}^{-1}$ one may put more stringent tolerances for losses. Subsidiary thermal flows on the low-temperature part of the cryogenic system, occurring due to radiation heating, may be rather essential. Thus, if during irradiation, continuous in time and uniform in length, one accepts proton losses determined in (10) (with the accepted magnet model, cooling system, thermal and physical parameters and $\theta = 10^{-3}$, $d = 0,15 \text{ cm}$, $B = 0$) the

occurring thermal loadings at the helium temperatures per metre of the magnet length are of the following approximate values:

$\xi' = 0,11$	0,20	0,42	0,85
$q, W \cdot m^{-1} = 140$	115	70	20

Apparently, condition (13) can easily be violated here, therefore a more detailed consideration is needed.

VII. CONCLUSION

Note that the reliability of the results obtained in the paper is different. Inaccuracy in defining the energy deposition field $\epsilon(\vec{r})$ under the given irradiation conditions must not exceed $\approx 100\%$. The irradiation conditions depending on the particle losses distribution at the future accelerator are not totally known in advance. Therefore the real picture of energy deposition at all the stages of the operation cycle is awaiting its further investigation.

The estimates of tolerances of losses presented in Section VI correspond to the model irradiation conditions, magnet construction and parameters, cooling system as these are accepted in the present paper. Only in the case of "instantaneous" proton losses ($\tau < 1$ msec) these data must be approximately adequate to the actual situations in the UNK superconducting ring. The calculated tolerances for losses at $\tau > 1$ msec and, consequently, heat flows in various specific cases can be applied only to estimate the order of the magnitude.

The most thorough analysis and optimization of the solutions from three viewpoints is required: proton losses distribution in the accelerator, SMS quench and the cryogenic system scheme. Special measures to protect the SMS from irradiation¹⁷⁾ are obviously to be taken. In the places of the localized losses¹⁷⁾ the cryogenic system and possibly the magnets themselves should be different than in the remaining part of the accelerator circumference.

The authors are deeply indebted to V.N.Lebedev and K.P.Myznikov for discussions and their support.

* * *

REFERENCES

- 1) The Energy Doubler, Batavia, 1976.
- 2) V.I.Balbekov et al. Preprint IHEP 77-110, Serpukhov, 1977

- 3) Superconducting Conversion on the ISR. Preprint CERN 77-20, Geneva, 1977.
- 4) V.V.Frolov, N.V.Mokhov, O.I.Pogorelko. Preprint ITEP-114, Moscow, 1975.
- 5) G.Restat et al. Preprint CERN, ISR-HA/75-20, 1975.
- 6) A.Van Ginneken. Preprint FNAL TM-685, Batavia, 1976.
- 7) L.N.Zaitzev. Preprint JINR P16-10480, Dubna, 1977.
- 8) A.G.Daikovsky, M.A.Maslov, N.V.Mokhov, A.I.Fedoseev. Preprint IHEP 77-139, Serpukhov, 1977.
- 9) N.V.Mokhov. Proceedings of IV All-Union Workshop on Charged Particle Accelerator, Moscow, 1974, v. II, M., "Nauka", 1975, p. 222.
- 10) N.V.Mokhov. Preprint IHEP 76-64, Serpukhov, 1976.
- 11) I.S.Baishev, S.L.Kuchinin, N.V.Mokhov. Preprint IHEP 78-2, Serpukhov, 1978.
- 12) A.S.Denisov et al. Preprint LINP N459, Leningrad, 1978.
- 13) M.A.Maslov, N.V.Mokhov, A.V.Uzunyan. Preprint IHEP 78-153, Serpukhov, 1978.
- 14) N.V.Mokhov. JTP, 49 (1979), 1254.
- 15) J.Allinger et al. Stability of High Field Superconducting Dipole Magnets. BNL, Brookhaven, 1977.
- 16) G.Brechna. Superconducting Magnet System. M., "Mir", 1976.
- 17) V.I.Balbekov et al. In abstracts of Contributions at VI All-Union Workshop of Charged Particle Accelerators. Dubna, 1978, p. 23. In Proc. Workshop Possib. Limitat. Accel. Detectors. FNAL, Oct. 1978. FNAL, April 1979, pp. 49-65.

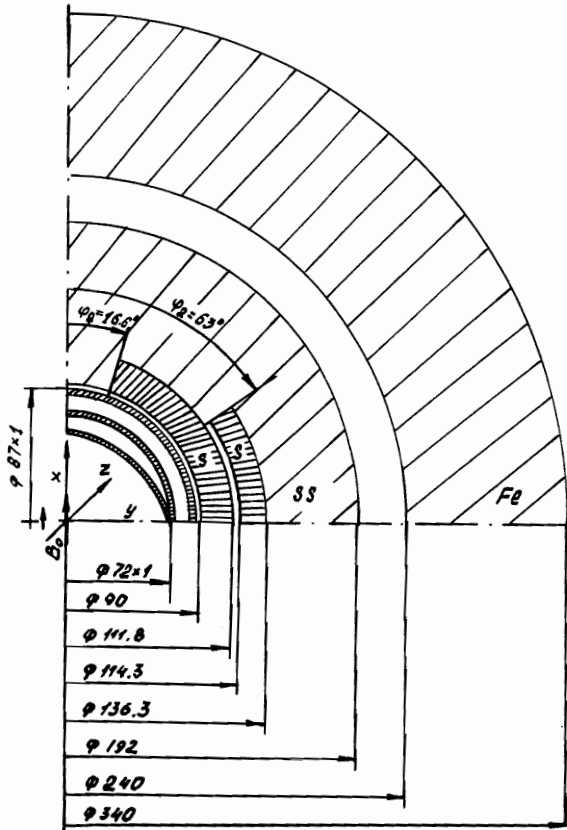


Fig. 1. The model of the UNK superconducting dipole magnet as it is accepted in the present calculation. S is the superconducting winding (SCW), SS is stainless steel (the bandage).

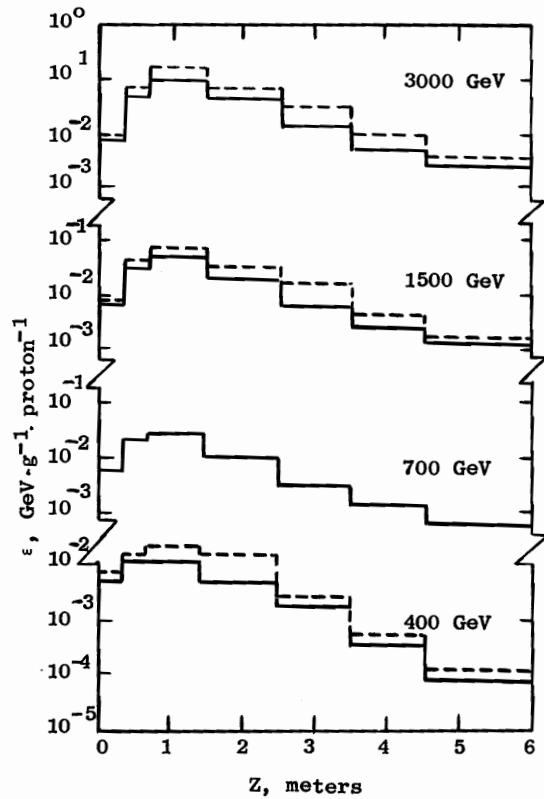


Fig. 2. The longitudinal distribution of the energy deposition density in the dipole magnet superconducting winding irradiated at the fixed angle $\theta = 10^{-3}$ to the vacuum chamber by a proton beam of various energies of infinitesimal lateral extent (case 1). $r = 4,5 - 5,1$ cm; $1,52 < \phi < 1,62$; — $B = 0$; --- $B = 5$ T.

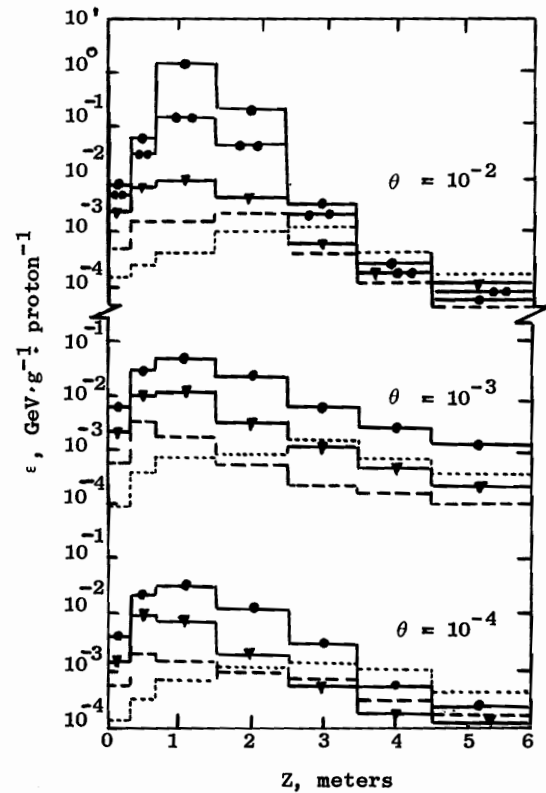


Fig. 3. The same as in the previous figure but for various angles θ and ϕ at $E_0 = 1500$ GeV and $B = 0$. —●— $1,52 < \phi < 1,62$; —●— $1,32 < \phi < 1,52$; —●— $0,92 < \phi < 1,32$; --- $0,52 < \phi < 0,92$; - - - - $4,66 < \phi < 4,76$.

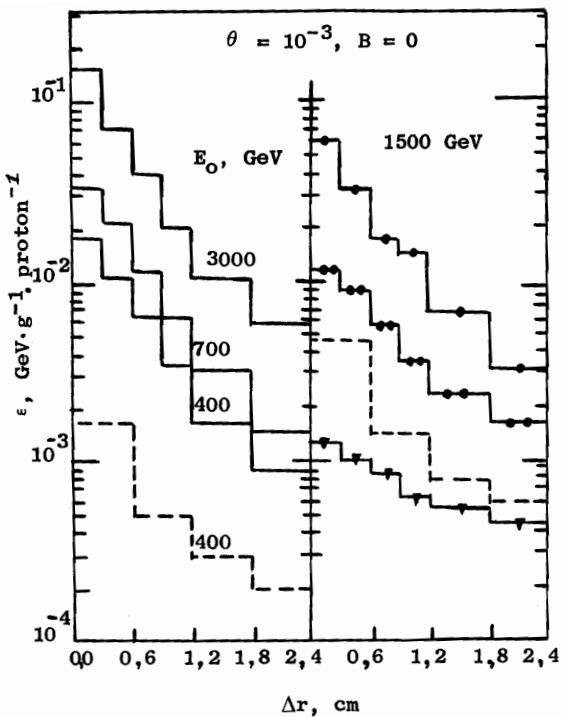


Fig. 4. The radial distributions of the energy deposition density in the dipole winding in the maximum of longitudinal distributions (case 1). $r = 4,5 - 6,9$ cm. On the left $1,52 < \phi < 1,62$. On the right \bullet $1,52 < \phi < 1,62$; \bullet $1,62 < \phi < 3,14$; \bullet $3,14 < \phi < 4,71$. The dashed histogram depicts the data (2) averaged in the azimuth.

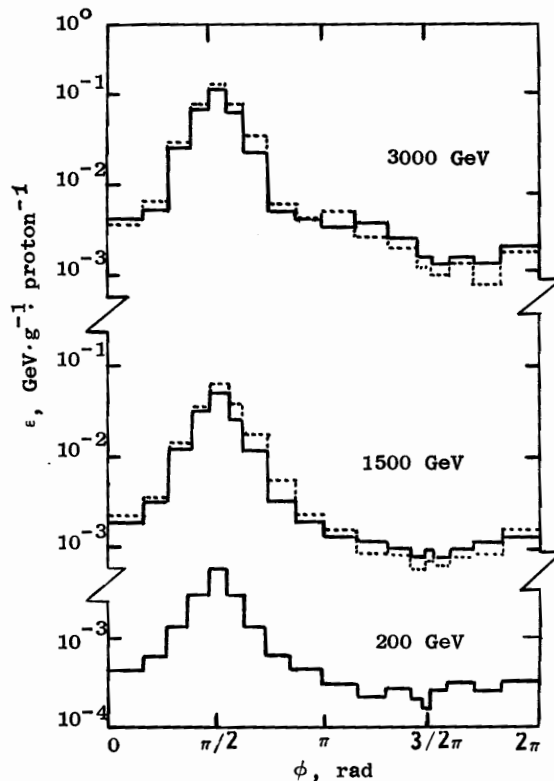


Fig. 5. The azimuthal distribution of the energy deposition density in the SCW in the cascade maximum with losses of a single proton beam of various energies (case 1). $r = 4,5 - 5,1$ cm $\theta = 10^{-3}$; — $B = 0$; - - - $B = 5$ T.

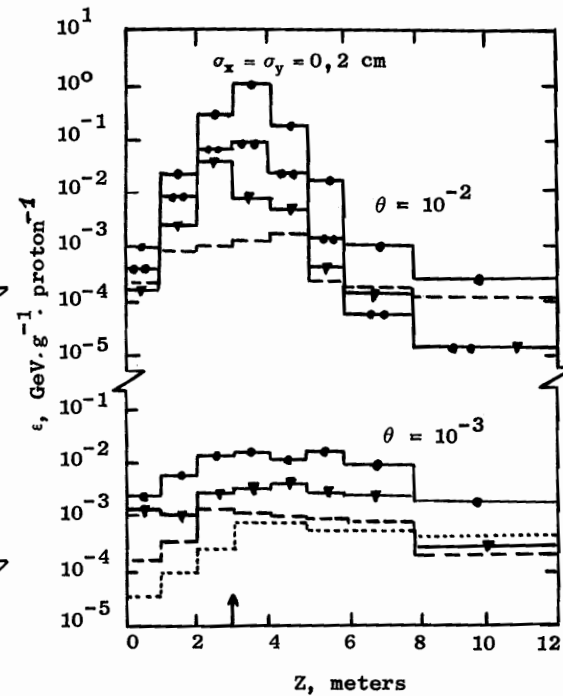


Fig. 6. The azimuthal distribution of the energy deposition density in the SCW with normally distributed losses (1) of a single proton beam (case 3). $E_0 = 1500$ GeV; $r = 4,5 - 5,1$ cm; $B = 0$; \bullet $1,52 < \phi < 1,62$; \bullet $1,32 < \phi < 1,52$; \bullet $0,92 < \phi < 1,32$; \bullet $0,52 < \phi < 0,92$; \bullet $4,66 < \phi < 4,76$. The arrow shows the position of the beam "centre of gravity".

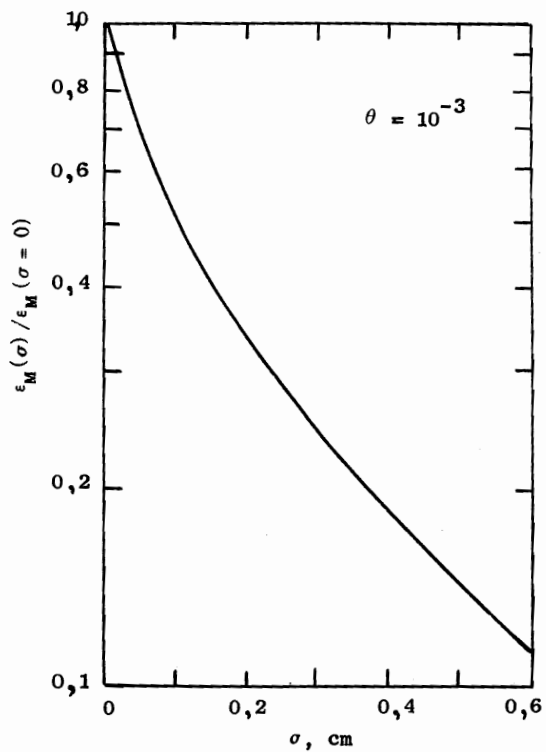


Fig. 7. The dependence of the maximum energy deposition density in the SCW on the dispersion of the proton beam density distribution at $E_0 = 200 - 300$ GeV. $B = 0$; $\theta = 10^{-3}$; $d = 0,15$ cm.

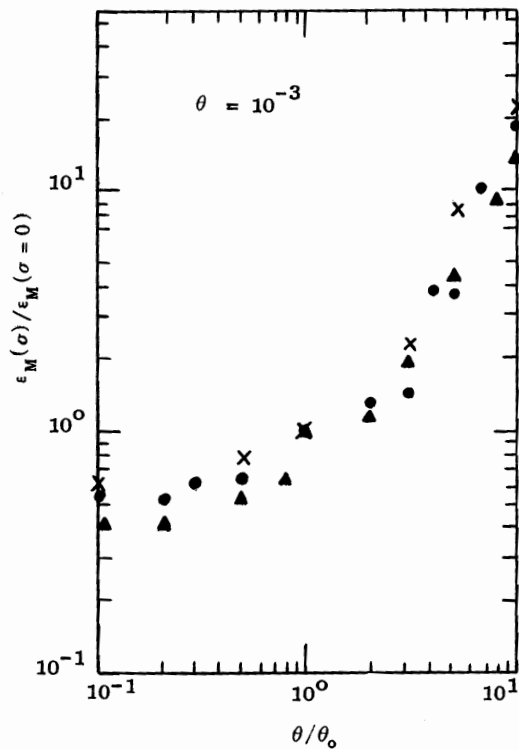


Fig. 8. The maximum energy deposition density in the superconducting windings as dependent on the proton incident angle on the vacuum chamber. $d = 0,15$ cm; $E_0 = 400 - 3000$ GeV. \bullet - case 1, $B = 0$, \blacktriangle - case 2. $B = 0$; \times = case 1, $B = 5T$.

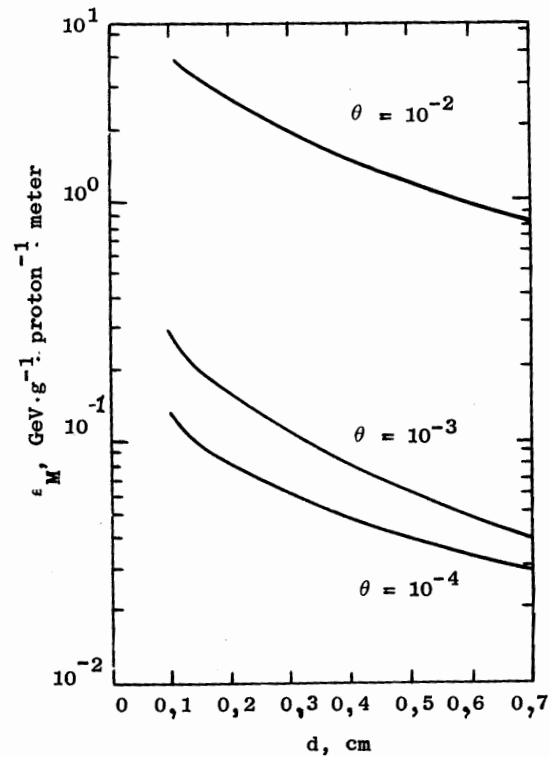


Fig. 9. The maximum energy deposition in the SCW as dependent on the total thickness of the "vacuum" chamber for various angles of incident protons on the chamber. $E_0 = 1500$ GeV; $B = 0$.

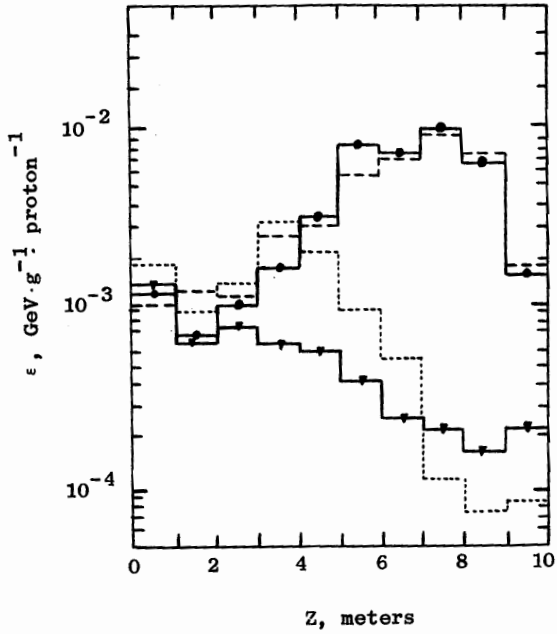


Fig. 10. The longitudinal distributions of the Doubler superconducting dipole winding. The distance between magnets and the target $D = 20$ m, $E_0 = 1000$ GeV; $r = 3,9-4,2$ cm. Our calculation is as follows:
 —●— $1,47 < \phi < 1,57$; $B = 4,2$; ... $4,61 < \phi < 4,71$, $B = 4,2$ T; —■— $B = 0$. The calculation in paper⁶):
 - - - - $1,47 < \phi < 1,57$; $B = 4,2$ T. The data have been normalized per one proton interacted with the target.

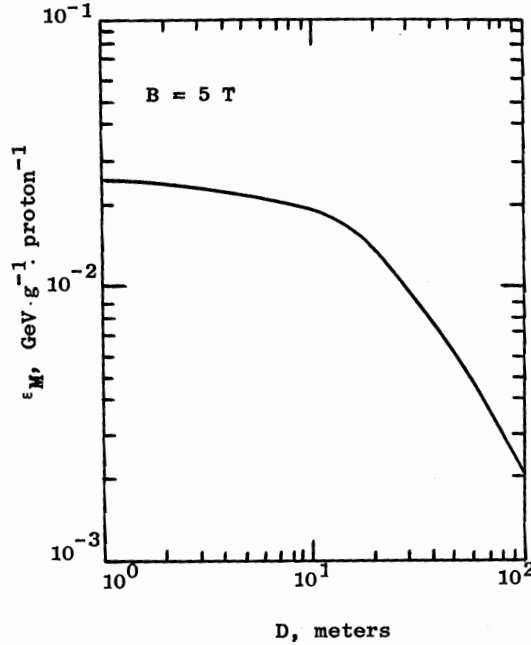


Fig. 11. The maximum energy deposition in the UNK as dependent on the distance between the magnet and the target interacted with a 1500 GeV proton.

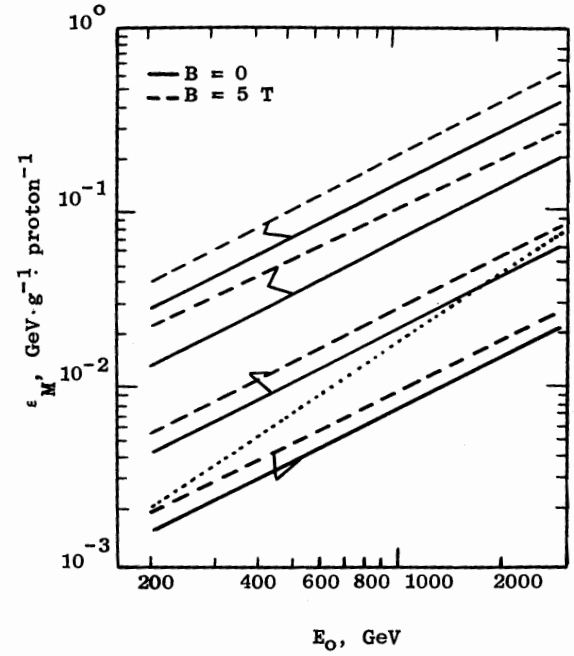


Fig. 12. The dependence of the maximum extrapolated energy deposition in the UNK dipole SCW on the energy of proton incident at $\theta = 10^{-3}$ on the vacuum chamber for various cases of irradiation. The data averaged in the azimuth are depicted by the dashed line. For case 2 and 2' the dimension $[\epsilon_M] = \text{GeV} \cdot \text{g}^{-1} \cdot \text{proton}^{-1} \cdot \text{m}$

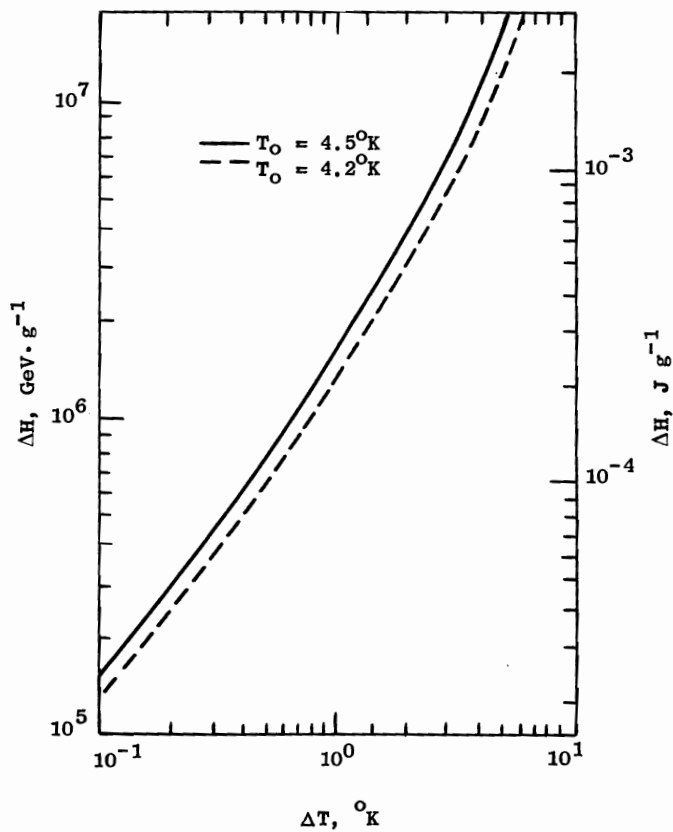


Fig. 13. The enthalpy for the superconducting winding material

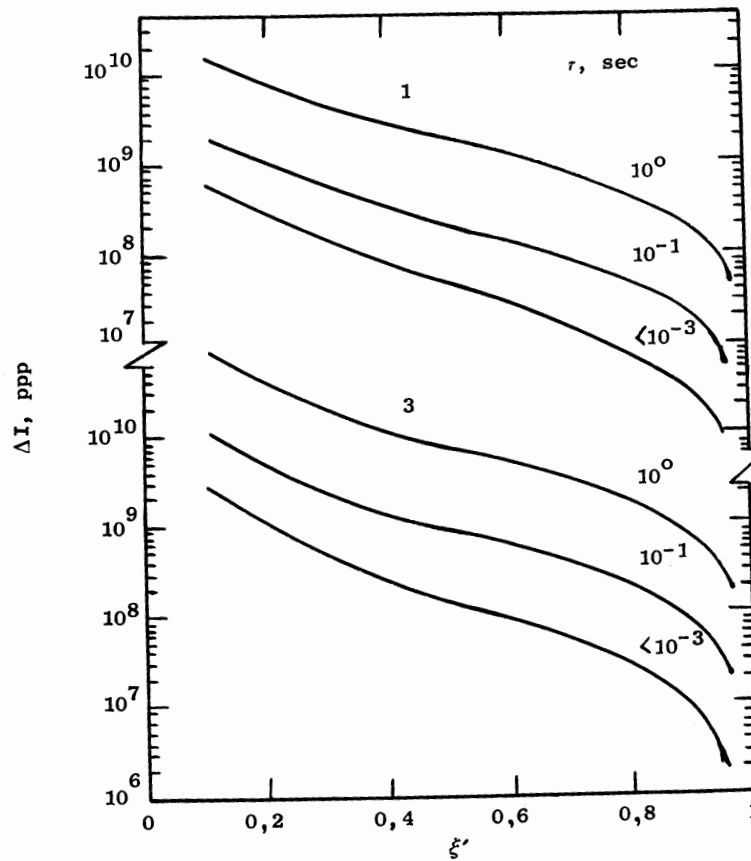


Fig. 14. The tolerable proton losses (cases 1 and 3) for the accepted magnet model with various duration of losses pulses. $\theta = 10^{-3}$.